



## Rapid Prototyping Journal

Structural optimization of printed structures by self-organized relaxation

Andrea Zocca Cynthia Gomes Ulf Linow Heidi Marx Jörg Melcher Paolo Colombo Jens Günster

### Article information:

To cite this document:

Andrea Zocca Cynthia Gomes Ulf Linow Heidi Marx Jörg Melcher Paolo Colombo Jens Günster , (2016), "Structural optimization of printed structures by self-organized relaxation", Rapid Prototyping Journal, Vol. 22 Iss 2 pp. 344 - 349

Permanent link to this document:

<http://dx.doi.org/10.1108/RPJ-07-2014-0087>

Downloaded on: 28 April 2016, At: 08:16 (PT)

References: this document contains references to 8 other documents.

To copy this document: [permissions@emeraldinsight.com](mailto:permissions@emeraldinsight.com)

The fulltext of this document has been downloaded 36 times since 2016\*

### Users who downloaded this article also downloaded:

(2016), "Direct digital manufacturing of an accelerator pedal for a Formula Student racing car", Rapid Prototyping Journal, Vol. 22 Iss 2 pp. 311-321 <http://dx.doi.org/10.1108/RPJ-05-2014-0065>

(2016), "Development of ABS based wire as feedstock filament of FDM for industrial applications", Rapid Prototyping Journal, Vol. 22 Iss 2 pp. 300-310 <http://dx.doi.org/10.1108/RPJ-07-2014-0086>

(2016), "Feature based building orientation optimization for additive manufacturing", Rapid Prototyping Journal, Vol. 22 Iss 2 pp. 358-376 <http://dx.doi.org/10.1108/RPJ-03-2014-0037>

Access to this document was granted through an Emerald subscription provided by

Token: JournalAuthor:E2053DA5-2345-4ED7-8A2A-CDC402187A05:

### For Authors

If you would like to write for this, or any other Emerald publication, then please use our Emerald for Authors service information about how to choose which publication to write for and submission guidelines are available for all. Please visit [www.emeraldinsight.com/authors](http://www.emeraldinsight.com/authors) for more information.

### About Emerald [www.emeraldinsight.com](http://www.emeraldinsight.com)

Emerald is a global publisher linking research and practice to the benefit of society. The company manages a portfolio of more than 290 journals and over 2,350 books and book series volumes, as well as providing an extensive range of online products and additional customer resources and services.

Emerald is both COUNTER 4 and TRANSFER compliant. The organization is a partner of the Committee on Publication Ethics (COPE) and also works with Portico and the LOCKSS initiative for digital archive preservation.

\*Related content and download information correct at time of download.

# Structural optimization of printed structures by self-organized relaxation

*Andrea Zocca*

Department of Ceramic Processing and Biomaterials, BAM Federal Institute for Materials Research and Testing, Berlin, Germany

*Cynthia Gomes*

Department of Materials Engineering, BAM Federal Institute for Materials Research and Testing, Berlin, Germany

*Ulf Linow and Heidi Marx*

Department of Ceramic Processing and Biomaterials, BAM Federal Institute for Materials Research and Testing, Berlin, Germany

*Jörg Melcher*

Institute of Composite Structures and Adaptive Systems, German Aerospace Center DLR, Braunschweig, Germany

*Paolo Colombo*

Dipartimento di Ingegneria Industriale, University of Padova, Padova, Italy, and

*Jens Günster*

Department of Ceramic Processing and Biomaterials, BAM Federal Institute for Materials Research and Testing, Berlin, Germany

## Abstract

**Purpose** – This paper aims to present an additive manufacturing-based approach in which a new strategy for a thermally activated local melting and material flow, which results in densification of printed structures, is introduced.

**Design/methodology/approach** – For enabling this self-organized relaxation of printed objects by the viscous flow of material, two interconnected structures are printed simultaneously in one printing process, namely, Structure A actually representing the three dimensional object to be built and Structure B acting as a material reservoir for infiltrating Structure A. In an additional process step, subsequent to the printing job, an increase in the objects' temperature results in the melting of the material reservoir B and infiltration of structure A.

**Findings** – A thermally activated local melting of the polymethylsilsesquioxane results in densification of the printed structures and the local formation of structures with minimum surface area.

**Originality/value** – The present work introduces an approach for the local relaxation of printed three-dimensional structures by the viscous flow of the printed material, without the loss of structural integrity of the structure itself. This approach is not restricted only to the materials used, but also offers a more general strategy for printing dense structures with a surface finish far beyond the volumetric resolution of the 3D printing process.

**Keywords** Printing, 3D

**Paper type** Research paper

## Introduction

Liquids in contact with solid surfaces show a wetting or dewetting behavior. Wetting describes the tendency of a liquid to maximize its interfacial area with a solid, which, however, must be always seen in competition to a concomitant expansion of other interfaces, e.g. the liquid – air interface. Liquids in contact with a gaseous medium generally tend to minimize their surface area, as locating a molecule at the gas–liquid interface is energetically less favorable than in the liquid volume. For liquids, the energy to create a unit area of surface is identical to the surface tension (force per unit length). The interplay between the energy gained by wetting a

solid surface and the energy required for expanding the gas – liquid interface determines the shape of a droplet supported by a solid surface. This well-known effect can be used as a measure for the surface tension of the supporting substrate when the surface tension of the liquid is known.

Apart from the wetting of flat substrates, liquid surfaces can form complex topologies in case additional geometrical constraints do exist. In this context, a simple example is a soap bubble: while the inner bubbles gas pressure keeps the object expanded, the surface tension of the bubble membrane establishes a three-dimensional surface with minimum area. By the interplay of inner gas pressure and surface tension, an ideal spherical object is formed. For the same reason, multiple soap bubbles in contact with each other can form rather complex geometries. Another example is a randomly shaped solid wetted by a liquid. The interplay between the energy gained by wetting the solids surface and the energy required for the formation of the liquid-air interface determines the

The current issue and full text archive of this journal is available on Emerald Insight at: [www.emeraldinsight.com/1355-2546.htm](http://www.emeraldinsight.com/1355-2546.htm)



Rapid Prototyping Journal  
22/2 (2016) 344–349  
© Emerald Group Publishing Limited [ISSN 1355-2546]  
[DOI 10.1108/RPJ-07-2014-0087]

Received 23 July 2014  
Revised 24 December 2014  
Accepted 9 February 2015

shape of the liquid phase. Because of the surface tension of the liquid, its surface will establish objects with minimum surface area locally. As a consequence, the thickness of the film formed will not be constant. Practically, this means that rough surfaces and sharp edges will be smoothed out. In this context, this work presents an additive manufacturing (AM)-based approach to initiate a self-organized relaxation of complex structured surfaces to locally form objects of minimum surface area.

AM describes a class of technologies in which a 3D object is directly generated from a virtual model by adding material in a layer-by-layer approach defined by ASTM F279 - 12a (Standard Terminology for Additive Manufacturing Technologies) as the “process of joining materials to make objects from 3D model data, usually layer upon layer, opposed to subtractive manufacturing methodologies, such as traditional machining” (ASTM International, 2010). The philosophy behind AM is simple: a virtual dataset and the choice of material are sufficient to build a part within a ubiquitous manufacturing process. The material is typically fed into the process as a powder, paste or liquid, that is, the material is in a state optimized for the layer deposition process, but not useful to defining a finite geometry. In the manufacturing process itself, the material is used to build up the desired object and is simultaneously transferred into a state showing its final physical properties or at least a mechanical strength sufficient to transfer the object built to further processing steps. In powder-based AM technologies, a solid structure is realized by the successive deposition of layers of a flowable powder. Briefly, a layer of powdered material is first spread and subsequently the corresponding layer information is selectively inscribed by, for example, local compaction or gluing; these steps are iteratively replicated until the object is completed. The layer information is defined by the corresponding cross-section of a sliced virtual 3D-model of the object to be built. At the end, the part is completely embedded in a powder bed, from which it can be easily extracted and cleaned. The technology used to inscribe the layer information depends on the specific process considered: two of the most well-known and world-spread processes are the “Three-dimensional printing (3DP)” (Sachs et al., 1993) and the “Selective laser sintering, (SLS)” (Deckard, 1989). The so-called “powder-based three-dimensional printing”, which has been used for the present work, is one of the most used AM technologies, and it is based on the concept that the powder in each layer is selectively bonded by the means of a printhead according to the corresponding slice of the computer-aided design (CAD) model. The printhead is locally jetting a binder into the powder layers to glue the powder particles together. Parts generated by 3DP are characterized by a high porosity, typically not below 50 per cent. Also, the definition of the parts shape is restricted by the size of the powder particles and the layer thickness. A good flowability of the powders in use is a prerequisite for a successful layer deposition. Hence, the powder particles are generally not significantly smaller than 50  $\mu\text{m}$  for polymeric and ceramic powders. The layer thickness is typically in the range of 50 to 100  $\mu\text{m}$ .

One major difference of AM in comparison to subtractive technologies is the fact that the manufacturing of

complex-shaped parts takes about the same time than the manufacturing of simple voluminous structures. Therefore, AM is well suited for the manufacture of porous ordered structures (three-dimensional lattice structures) for lightweight constructions. Diamond or Kagome (Lee et al., 2007; Wang et al., 2003) structures are examples of a class of highly porous structures with optimized mechanical properties (Figure 1). The mechanical properties of these structures are ultimately defined by the mechanical properties of the filigree network of struts forming the solid structure. For load-bearing applications, the individual struts must be dense and should ideally show a smooth surface. Both of these requirements are not easily satisfied by 3DP. The present approach, on the other hand, introduces a new strategy in which a thermally activated local melting of printed structures initiates an effective material flow, resulting in an *in situ* densification of the struts and the formation of an ideally smooth surface. Moreover, the viscosity of the printed structure can be reduced to an extent, enabling the local formation of structures with minimum surface area.

As a model material, a commercially available powder of a polymethylsilsesquioxane preceramic polymer, with the brand name of MK, from Wacker Chemie (Burghausen, Germany) has been used.

Thermal cross-linking is usually carried out on the molten polymer of MK at temperatures of more than 100°C; however, it has been proved in a previous work that if the heating rate is slow enough, it is possible to cross-link the material starting from room temperature already before reaching  $T_g$ , when a catalyst is present (Zocca et al., 2013). This is very important for parts shaped by powder-based 3DP, because the process is carried out at room temperature and the shape has to be kept during the subsequent heat treatment that is performed to convert the preceramic polymer object into a ceramic one. After cross-linking, the preceramic polymer can in fact be transformed into a ceramic material by pyrolysis in an inert atmosphere. The polymer to ceramic transformation is well-known and beyond the scope of the present work.

## Experimental

For 3DP, a polymethylsilsesquioxane powder was used (Silres MK polymer, Wacker Chemie, Burghausen, Germany). This

**Figure 1** Octahedra structure printed from Wacker MK preceramic polymer (after pyrolysis)



preceramic polymer, in the following designated as MK, was chosen because it is commercially available, inexpensive and provided as a fine powder. The pure MK polymer has a softening temperature of 45–60°C, but it can be cross-linked by catalyzed polycondensation of hydroxyl and ethoxyl groups (which are present approximately in 2 mol per cent) (Harsche et al., 2004).

A simple approach was followed to introduce the cross-linking catalyst in the powder: tin-octoate (TinOc) (Sigma Aldrich, Hannover, Germany), which is a liquid, was mixed directly with the solvent printed into the powder. As a solvent, a mixture of 1-hexanol and hexylacetate (Voxeljet, Augsburg, Germany) (the mixture will be called “hexanol mixture” from here on) was chosen. This strategy allowed to introduce the catalyst directly during the printing job.

A ratio of catalyst/(catalyst + solvent) = 7.6 wt% was chosen as also used in a previous work (Zocca et al., 2013). Details can be found in the reference and here only the most important details and modifications will be discussed. This mixture enabled the introduction of 0.9–1 wt% of catalyst into the printed powder. In this case, the pure as received MK powder was sieved to remove the smaller and the bigger fractions to improve the flowability and make it fit for the layer-by-layer deposition. The main properties of the resulting powder are presented in Table I.

The flowability of the powder was evaluated by the Hausner ratio (H), measured according to equation (Hausner, 1981):

$$H = \rho_{\text{Tapped}} / \rho_{\text{Bulk}} \quad (1)$$

where  $\rho_{\text{Bulk}}$  is the freely settled bulk density of the powder, and  $\rho_{\text{Tapped}}$  is the plateau density of the tapped powder after a certain number of standardized tapping cycles.

The printer used was a Voxeljet VTS 16 machine (Voxeljet Technology GmbH, Friedberg, Germany) equipped with two printheads with 128 jets (Spectra SL128-AA, Dimatix Fujifilm, USA) and using a blade recoating system.

The ratio (R) between the mass of solvent and the mass of powder in a printed part is a critical parameter for obtaining stable parts. As a printed object can be considered to be a repetition of a single voxel (the three dimensional equivalent of a pixel) and since the printhead ejects one drop of solvent for each voxel, R is then equivalent to the mass of a single drop divided by the mass of powder in one voxel, according to equation (2):

$$R = (\text{drop mass}) / (dx \cdot dy \cdot dz(\rho_{\text{Bulk}})) \quad (2)$$

where  $dx \cdot dy$  is the lateral pixel area of the substrate on which one droplet is ejected and  $dz$  is the layer thickness; the value  $dx \cdot dy \cdot dz$  is therefore the volume of one voxel.

**Table I** Particle size distribution, bulk density and Hausner ratio of the polymethylsilsequioxane powder after sieving

D10 ( $\mu\text{m}$ )	D50 ( $\mu\text{m}$ )	D90 ( $\mu\text{m}$ )	D97 ( $\mu\text{m}$ )	Bulk density ( $\text{g}/\text{cm}^3$ )	Hausner ratio <sup>a</sup>
4	3	08	41	0.535	1.25

**Note:** <sup>a</sup>HR < 1.11 = excellent flow; 1.12–1.18 = good flow; 1.19–1.25 = fair flow; 1.26–1.34 = passable flow; 1.35–1.45 = poor flow; 1.46–1.59 = very poor flow; >1.60 = no flow

The mass ratio between catalyst and MK powder in a printed part can be calculated from the following equation (3):

$$\begin{aligned} & \text{catalyst/MK wt\%} \\ &= (\text{catalyst in 1 voxel}) / (\text{powder in one voxel}) \\ &= (\text{drop mass } 7.6/100) / (dx \cdot dy \cdot dz (\rho_{\text{Bulk}})) \\ &= R \cdot 7.6/100 \end{aligned} \quad (3)$$

The printed parts were left immersed in the support powder bed overnight to evaporate the excess solvent and were finally cleaned by means of a brush and a compressed air gun.

The green parts were typically cross-linked by slowly (1.5°C/h) heating them up to 70°C with a dwelling time of 1 h in a heating cabinet with forced air circulation (Type TR 60, Naberherm GmbH, Bremen, Germany). To decrease the influence of the gravitational force on the parts during thermal treatment and to favor the self-organization processes, complex-shaped parts were immersed into water during the heat treatment. As the difference in density between the polymer ( $\rho = 1.2 \text{ g}/\text{cm}^3$ ) and water is small, the resulting force (sum of Archimedean force and gravitation) acting on the part immersed in water is much smaller than if the part was subject to gravitation alone. Because of the hydrophobic nature of the MK material, water did not penetrate the pores of the printed part.

The morphology of the printed parts was investigated using an optical microscope (VHX-100 digital microscope, Keyence corporation, Japan) and scanning electron microscopy (SEM; JEOL JSM-6490, Jeol Italia, Pieve Emanuele (MI), Italy).

## Results and discussion

For enabling a self-organized relaxation of printed objects by the viscous flow of a material, two interconnected structures were printed simultaneously in one printing process: Structure A actually representing the three dimensional object to be built and Structure B acting as a material reservoir. In the following, both structures are designated as Structure A and B. In an additional process step, subsequent to the printing job, an increase in the objects' temperature resulted in the melting of the material reservoir B and the *in situ* infiltration of Structure A.

To introduce this strategy, a core-shell structure was generated in the 3DP process by using the Wacker MK polymer powder. In the printing process, the MK polymer powder was consolidated by printing a solvent, the “hexanol mixture” (see experimental section), in selected areas of each layer. The “hexanol mixture” acts as a solvent for the MK powder, and the consolidation of the powder is achieved by partially dissolving the powder particles. This dissolution enables mobilization of the material by viscous flow and results in the compaction of the powder and interconnection of the particles. The mobilization of the material is evidenced by densification of the powder in the areas on which the “hexanol mixture” was printed, from initially 45 per cent to about 80 per cent theoretical density. As the printer is equipped with two printheads, two printing liquids could be used simultaneously in one print job: the pure “hexanol mixture” and the “hexanol mixture” containing 7.6 wt% cross-linking catalyst. In each layer, therefore, two distinct regions were treated independently, one corresponding to



Structure A, the supporting skeleton of a three-dimensional lattice structure (core), and one corresponding to Structure B, the material reservoir for infiltration (shell). In this example, Structure A forms an inner skeleton wrapped up by Structure B. Structure A was printed using the “hexanol mixture” containing the cross-linking catalyst, while Structure B was printed using the pure “hexanol mixture”. Figure 2 shows both structures, which have been drawn with commercial CAD software (Solid Edge ST3, Siemens PLM Software Germany, Köln).

Figure 3 shows the printed part. Typical to parts generated by 3DP is a high porosity. As already mentioned, because of the use of a solvent, the MK powder could be consolidated to a density of about 80 per cent, while the density of the deposited powder layers did not exceed 45 per cent. Because of the porosity of the parts and the resulting scattering of visible light, the parts appear white.

After the part was printed, the entire structure was placed into the heating cabinet. To initiate cross-linking of the core and the melting of the shell structure, the temperature in the heating cabinet was ramped very slowly. This ensured that the cross-linking of the core structure would occur before the shell structure started melting. In fact, if the shell would melt too quickly, the entire structure would collapse.

After the thermal treatment, the structure shown in Figure 4 was obtained. For the sake of clarity, Figure 5 provides an overview of the described procedure in a process flow diagram.

Instead of a part which is formed by individual particles glued to each other, the structure now comprises compact and transparent regions with smooth surfaces. A closer inspection of the part reveals two distinct regions: regions formed by fully dense and transparent material and translucent regions with a rougher surface.

During heating, Structure A, which was printed with the catalyst, started to cross-link. During cross-linking, no significant densification of the part was observed. Parts which were printed using the cross-linking catalyst only did not change their density and outer contour during thermal treatment. In the present case, however, Structure A forms a skeleton (core) which is contained within a shell Structure B, which was printed without catalyst. Therefore, at a temperature of about 50°C ( $T_g$  of the MK), the shell started to melt and flow. As core and shell are made of the same material, the melting shell was able to wet the rigid material of the core structure and finally infiltrated the porous core, with infiltration driven by capillary forces.

**Figure 2** Structures modeled for 3D printing: Structure A, inner skeleton (core), left, and Structure B (shell, material reservoir), right

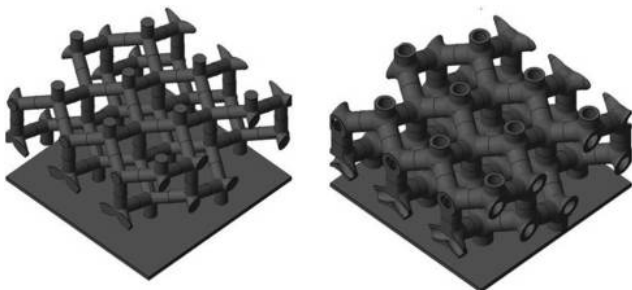


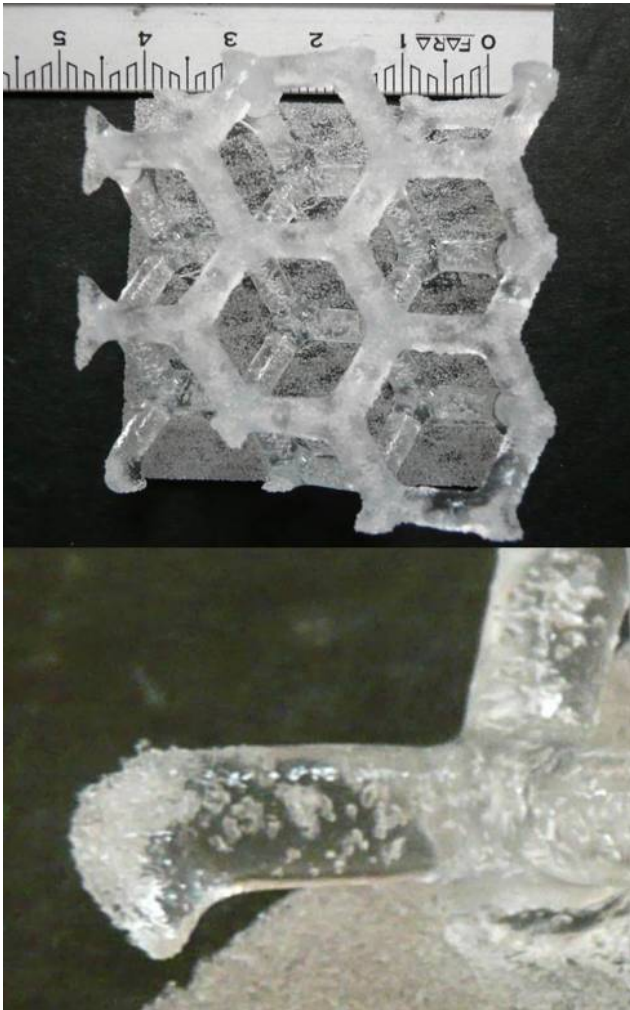
**Figure 3** Printed part comprising two structures: A the inner skeleton (core) and B the shell (material reservoir)



In these experiments, the core was completely surrounded by the shell structure; this design is not optimal for a bubble-free infiltration of the core. Gas in the porous core can easily remain entrapped by the melting shell, as infiltration of the core is subsequent to the melting of the shell. Entrapped gas was concentrated in bubbles in the middle of the strut structures, and the bubbles inner gas pressure would finally hamper complete infiltration.

The volume of the shell structure B ultimately defines the amount of liquid phase available for infiltration during thermal treatment. Driven by capillary forces, the liquid material is dragged into the pores of the core structure until the core is completely infiltrated. In case sufficient material for a complete infiltration of the core is available, surplus liquid phase will form a smooth surface. The smoothness of the surface is a result of the surface tension of the liquid MK phase. If sufficient liquid phase is not provided for the full infiltration of the core, the core will be infiltrated partially and

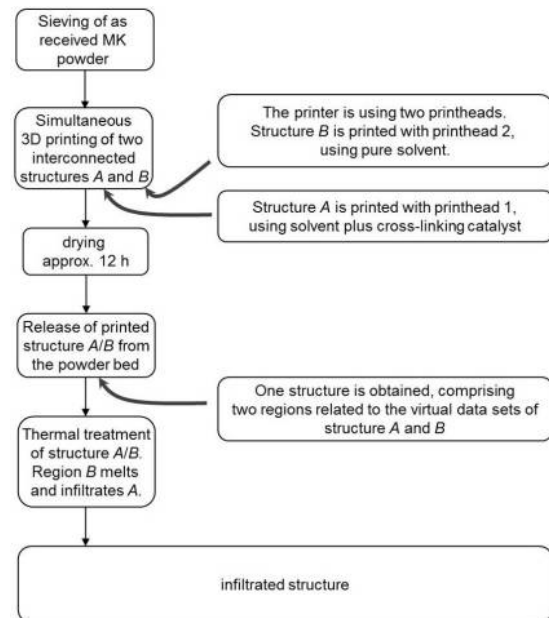
**Figure 4** Printed part from Figure 3, after thermal treatment up to 70°C



the surface remains rough. In the present case, we can estimate that about 50 per cent of the surface remained rough, indicating that the amount of liquid phase was not sufficient to fully cover the structure with a liquid film. In this context, it is noteworthy to observe that the capillary forces were definitely higher than the forces provided by the surface tension of the air–liquid interface of molten MK. The capillary force is inversely proportional to the capillaries radius, which is equal to the pore radius in the present experiment.

Attempts to quantify the infiltration of printed and cross-linked MK bodies by molten MK were carried out by using an IMeter (MSB Breitwieser, Augsburg, Germany), but the high viscosity of the molten MK made it impossible to measure the rising meniscus of the liquid column. Particularly, the time required for infiltration would be a valuable parameter for optimizing the thermal treatment of printed bodies. On the other hand, it became obvious that dipping printed filigree structures of fully cross-linked MK into molten MK is not an alternative for the approach introduced by the present work. Bearing in mind that printed filigree structures are very fragile, the filigree will be destroyed by the acting forces during dipping. Furthermore, the space between the

**Figure 5** Process flow diagram for printing one Structure A/B comprising two regions A and B, while B can infiltrate A



struts will be completely filled with the liquid phase, which would be impossible to remove afterward. Therefore, the proposed approach of printing the liquid reservoir together with the structure to be infiltrated is not only saving a process step, but also offers a unique flexibility in tailoring the amount of liquid phase which is locally offered for infiltration.

## Conclusion

The present work introduces an approach for the local relaxation of printed three-dimensional structures by the viscous flow of the printed material, without the loss of structural integrity of the structure itself. A thermally activated local melting of the MK results in densification of the printed structures and the local formation of structures with minimum surface area. For enabling this self-organized relaxation of printed objects by the viscous flow of material, two interconnected structures are printed simultaneously in one printing process: Structure A actually representing the three-dimensional object to be built and Structure B acting as a material reservoir for infiltrating Structure A. This approach is not restricted to the material system used, but offers a more general strategy for printing dense structures with a surface finish far beyond the volumetric resolution of the 3DP process.

## References

- ASTM International (2010), *ASTM F2792-09e1 Standard Terminology for Additive Manufacturing Technologies*, ASTM International, Pennsylvania.
- Deckard, C.R. (1989), "Inventor; Board of regents", The University of Texas System, Assignee, Method and apparatus for producing parts by selective sintering, US Patent 4,863,538, Austin, 5 September.

- Harsche, R., Balan, C. and Riedel, R. (2004), "Amorphous Si(Al)OC ceramic from polysiloxanes: bulk ceramic processing, crystallization behavior and applications", *Journal of the European Ceramic Society*, Vol. 24 Nos 10/11, p. 3471.
- Hausner, H. (1981), "Powder characteristics and their effect on powder processing", *Powder Technology*, Vol. 30 No. 1, p. 3.
- Lee, Y.H., Lee, B.K., Jeon, I., Kang, K.J. (2007), "Wire-woven bulk Kagome truss cores", *Acta Materialia*, Vol. 55 No. 1, pp. 6084-6094.
- Sachs, E.M., Haggerty, J.S., Cima, M.J. and Williams, P.A. (1993), "Inventors; Massachussets Institute of Technology, Assignee", Three-dimensional printing techniques, US Patent

- 5,204,055; 20 April 1993, US Patent 5,204,0551993, Massachussets.
- Wang, J., Evans, A.G.K. and Dharmasena, H.N.G. (2003), "Wadley: on the performance of truss panels with Kagomé cores", *International Journal of Solids and Structures*, Vol. 40 No. 1, pp. 6981-6988.
- Zocca, A., Gomes, C.M., Staude, A. and Bernardo, E. (2013), "Jens Günster and Paolo Colombo: SiOC ceramics with ordered porosity by 3D-printing of a preceramic polymer", *Journal of Materials Research*, Vol. 28 No. 7, pp. 2243-2252.

### Corresponding author

Jens Günster can be contacted at: [jens.guenster@bam.de](mailto:jens.guenster@bam.de)